Potential Oscillations in Cellular Automaton Based Model for Passivation of Metal Surface

Jan Stępień[1(✉)] and Janusz Stafiej[2(✉)]

[1] Department of Complex Systems and Chemical Information Processing, Institute of Physical Chemistry, Polish Academy of Sciences, ul. Kasprzaka 44/52, 01-224 Warsaw, Poland
jstepien@ichf.edu.pl

[2] Department of Mathematics and Natural Sciences, Cardinal Stefan Wyszyński University, ul. Wóycickiego 1/3, Warsaw, Poland
j.stafiej@uksw.edu.pl

Abstract. Cellular Automata based approach to modelling of the corrosion and passivation of metals in electrolytes is presented. We simulate the growth of the passive layer using an asynchronous CA, implemented for parallel processing on a GPU. In the present version of our model, the studied system is under galvanostatic control. The electric potential is adjusted to fix the current flow to a prescribed value. In the electrochemical experiments, this leads to potential oscillations for certain values of the current. This is related to the fact that for certain range of potentials our system displays a negative differential resistivity. We manage to obtain potential oscillations in our simulations. To our knowledge this is the first time that this peculiar feature of passivating system is reproduced by a computer simulation.

Keywords: Corrosion · Passivation · Diffusion · Oscillations
Modelling · Parallel computing · Block-synchronous automata
Asynchronous cellular automata · Stochastic cellular automata

1 Introduction

This paper is devoted to modelling of the corrosion and passivation of metals. Many metals tend to corrode via electrochemical oxidation, particularly when in contact with electrolytes. Depending on the conditions, such corrosion may lead to creation of a passive layer on the metal surface [20]. This layer can be composed of weakly soluble corrosion products, including metal oxides, hydroxides and salts. Passivation slows corrosion down by a large factor. As the experiments have shown [11,12,15–17], it is possible to control whether, and how fast passivation occurs. The passive layer thickness and morphology can also be regulated. Passivation is strongly influenced by a constant or time dependent electric potential applied to the piece of metal, passing electric current through the surface, or by modifying the composition of the solution.

G. Mauri et al. (Eds.): ACRI 2018, LNCS 11115, pp. 92–101, 2018.
https://doi.org/10.1007/978-3-319-99813-8_8

We have been studying passivation in electrolyte solutions for many years, by means of simulations with stochastic asynchronous cellular automata. Our research so far [5,6,19] was focused on passivation in potentiostatic conditions, that is – with constant electric potential applied to the metal. In this paper, some results for passivation in galvanostatic conditions are presented. Connecting the passivating metal to a galvanostat may induce oscillations of the potential, and our simulations manage to reproduce such oscillations.

The simulations can help us understand the physico-chemical mechanism of passivation better, than using only experiments. Besides, they allow us to regulate any parameters of the system at will, particularly those that are not amenable to experimental control. Thus we can separate some features that have to be unseparated in the real world experiments. Furthermore, they may provide us with advice on how to control the morphology of passive layers, possibly including formation of interesting nanostructures. One example is the emergence of nanopores on titania or alumina [3,4,21] – hypothetically it could be possible to obtain similarly regular patterns on valve metals.

We are using CA in our work for a few reasons. Firstly, they find their use as general (toy) models applicable to wide classes of systems that have common features. Further, CA are often adequate models for complex phenomena. This is largely for efficiency reasons. In many cases molecular-scale simulations or differential equations are associated with unreasonably high computational costs. Corrosion is one of those complex phenomena – it is an inhomogenous system, involving many components and an unobvious interaction between reaction and diffusion. Finally, CA can be translated to parallel algorithms in a straightforward manner, and those algorithms will typically make use of multiprocessor hardware with high efficiency. In our work, graphics processing units (GPUs) are used for computation. Note that parallelization becomes slightly less trivial in cases where the choice is taken to employ an asynchronous CA, instead of a classic, synchronous one. This is the case for the model described here. Still, the solutions for the problems that arise can be found in the literature, e.g. in [1,2].

The CA-based models have found many applications in physical chemistry and related fields – including electrochemistry [13], corrosion science [7], materials science and metallurgy [8–10,14].

The rest of this paper is structured as follows: The *Model* section presents the CA model used for the simulations. It is discussed in which ways the model accounts for the particular physico-chemical phenomena, and how is it implemented for parallel execution. The *Simulations, Results and Discussion* section describes for which parameter vectors the simulations were conducted, what data was collected and how was it processed. After that, the most important results are presented, along with discussion. The article is summarized in *Conclusions*.

2 Model

The model of passivation presented here is the same as in our publications on the passivation in potentiostatic conditions [5,6,19]. This is why only a short

description is presented in this section. The reader can find more details elsewhere. The new aspect is the galvanostatic control over the system.

The model is kept as general and simple as possible. It contains only the ingredients that are essential for reproducing the salient features of passivation. Corrosion and passivation works in similar ways for many different metals. This model assumes a metal with chemical properties similar to those of iron or other valve metals.

2.1 Physicochemical Basis of the Model

The model includes three processes that are responsible for the passive layer formation. The first of them is electrochemical oxidation of metal at its surface, caused by a corrosive environment. The rate of oxidation of exposed metal is a function of electric potential applied to the metal. The overall rate of corrosion depends also on the degree of passivation (coverage by the products of corrosion) and it is directly proportional to the current flowing through the system. In this model, we assume that the metal is connected with a galvanostat, therefore the potential is continuously regulated in an effort to keep the current constant. It should be emphasized, that the current cannot be controlled directly. Even with the best galvanostat, the current will be subject to random fluctuations. What is more, the maximum current in the studied system is limited by passivation. If the desired current value is too high, it is not possible to maintain it by galvanostatic control. In such a situation, the galvanostat will eventually output the highest potential available. The condition, when increasing the potential leads to a decrease in the current, is called negative differential resistivity.

The second modelled process is the precipitation of insoluble corrosion products on the metal surface and formation of a compact passive layer. For the passivation to occur, the corrosion product has to be hardly soluble. It has to adhere to the metal surface, as well as to itself. This is modelled by the random walk with asymmetric exclusion that mimics diffusion of the oxide to solution and its surface rearrangement. Passivation is never perfect – even with the surface fully covered with the oxide, a small current keeps flowing. In our study, this is made possible by a symmetry of oxide and solution in asymmetric exclusion. If the oxide particles can enter the solution, then in the same way solution inclusions can move into the oxide layer. This sustains a growth of the layer even when it becomes compact. The solution inclusions behave in an analogous way as the ionic vacancies postulated by Macdonald [18].

If only those two processes are taken into account, infinite growth of the passive layer becomes possible, although the growth rate will converge to zero as the layer's thickness increases. To limit the oxide layer thickness, we have included a mechanism of irreversible dissolution of oxide. This enables the system to achieve a steady state (equilibrium), when the rate of the irreversible dissolution balances the oxide production.

2.2 Specification of the Automaton

The CA used for the simulations is stochastic and asynchronous. The lattice is three-dimensional, cubic, with periodic boundary conditions. The neighbourhood is that of von Neumann. There are three cell states postulated: metal (MET for short), aqueous solution SOL, and metal oxide OXI. In the initial state, the bottom 40% of the lattice is filled with metal, with the upper part containing solution. The transition rule is composed of three transitions:

1. Metal oxidation: MET + SOL → OXI + OXI
   It can occur for a MET cell which is in contact with the solution, i.e. has at least one SOL neighbour.
2. Oxide diffusion (random walk): OXI + SOL → SOL + OXI
   Possible for an OXI cell which is in contact with the solution.
3. Oxide dissolution: OXI → SOL
   Considered only for an OXI cell whose all neighbours are SOL.

The automaton is stochastic, which means that the transitions listed above occur with certain probabilities, discussed below. The model has four parameters: P_{break} influences the oxide diffusion by regulating its adhesion to itself and the metal, P_{die} regulates the oxide loss via dissolution, R_{dif} and I_{GS} characterize the operation of the galvanostat.

The probability P_{corr} of an oxidation event depends on the potential V via the function:

$$P_{corr} = \frac{\exp(V)}{1 + \exp(V)} \tag{1}$$

which is plotted in Fig. 1. The probability P_{swap} of a diffusion event is dependent on $-n_{broken}$, the change in the number of MET and OXI neighbours of the OXI cell being moved. If $n_{broken} \leq 0$, then $P_{swap} = 1$. Otherwise, $P_{swap} = P_{break}^{n_{broken}}$, where P_{break} is a model parameter. The probability P_{die} of oxide dissolution is another parameter. If a MET is considered for dissolution, and it is stochastically chosen not to occur, then diffusion is considered immediately.

Electric potential V is adjusted by the galvanostat after each time step, in order to keep the actual current as close as possible to the set value. This is done using the following formula:

$$V_t - V_{t-1} = -R_{dif}(I_{t-1} - I_{GS}) \tag{2}$$

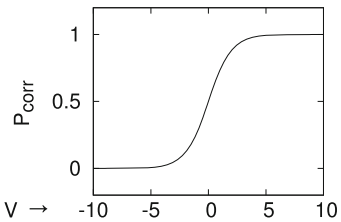

Fig. 1. Corrosion event probability P_{corr} as function of the potential V.

where V_t and I_t are respectively potential and current values during the time step number t, R_{dif} is the galvanostat's sensitivity factor, and I_{GS} is the desired current. Here, current is defined as the number of oxidation events per time step. Note that the state of the system is described by the states of the cells, and additionally a global variable V. Therefore, the initial V value also has to be specified.

2.3 Parallel Implementation

Due to the efficiency reasons, the lattice size has to be reasonable. In our case, it hardly ever exceeds $2048 \times 2048 \times 64$. We approximate studying a part of a much larger system by using periodic boundary conditions for the x and y directions. For z direction, it is assumed that the bulk solution extends to $+\infty$, and the bulk metal to $-\infty$. This condition is handled by introducing a scrolling mechanism. Every time when the corrosion consumes a metal volume corresponding to a single layer of cells, a monolayer is removed from the top of the lattice, and a monolayer of metal is appended to the bottom. When an oxide particle would diffuse past the z-extent of the lattice, it is annihilated (turned to SOL) instead. This method makes it possible to run a simulation for an arbitrarily long time.

Employment of a traditional, synchronous CA with the transition rule given is not possible without substantial changes to the model, because oxidation and diffusion transitions affect not just one cell, but also a randomly chosen neighbour. Therefore, as it has been mentioned, we decide to use an asynchronous automaton. In this case, an order of considering the cells for updating has to be given. To efficiently use the parallel processing capability of the GPUs, we have implemented our algorithm as a block-synchronous automaton, similar to those described in [1]. The only difference is that sampling with replacement is used in our case. The block size is set to 4^3.

The algorithm for the simulation, therefore, is as follows:
Until the desired simulation time is reached, do:

- for 64 times (block size):
  - Randomly choose a position in the unit block;
  - For the cell in that position, in every block: (the parallel part)
    - Choose a random neighbour (relevant for an oxidation or diffusion event);
    - Choose a transition based on the cell and selected neighbour's states – oxidation for MET and SOL, dissolution for OXI with only SOL neighbours, do nothing for SOL;
    - Randomly (with given probability) decide, whether the transition happens;
    - If the cell is OXI and dissolution has not been performed, consider diffusion next;
    - If a transition is chosen to be performed, update the cell(s) affected;
- If an equivalent of a monolayer of metal has been oxidized since last scrolling: Scroll by removing the top monolayer of the lattice and adding a monolayer of MET at the bottom;

– Compute the potential V for the next step (Galvanostat)

3 Simulations, Results and Discussion

The simulations are conducted to check the influence of all parameters. The sets of values for every parameter are selected based on initial test simulations, the earlier results presented in [19], and on the authors' intuition.

Instead of bare I_{GS} (current setting) and R_{dif} (galvanostat sensitivity), we used respectively I_{GS}/A and $R_{dif} \cdot A$ as parameters, where A is the area of the horizontal section of the lattice, $dim_x \cdot dim_y$ (all dimensions are in cells). Adopting this convention makes the system's behavior independent of the lattice size, if it is sufficiently large. To determine the appropriate size for further simulations, the impact of the lattice size was examined. First, the horizontal (dim_x and dim_y) dimensions from range 96–4096 were checked, with the lattice height (dim_z) = 96. Next, $dim_x = dim_y = 1024$ were assumed and dim_z was varied from 8 to 144. The other parameters were: $P_{break} = 0.15$, $P_{die} = 0.01$, $I_{GS}/A = 0.0002$ and $R_{dif}A = 200$. Those values had been found to cause nice potential oscillations (see Fig. 2, discussed later). The simulation time was 40000 steps. We found that for most of the following simulations, $dim_x = dim_y = 1536$ and $dim_z = 64$ are sufficient. For the cases when very small I_{GS}/A values were chosen, we extended dim_x and dim_y to 2048. This was meant to reduce the content of the random noise in the observed current.

The impact of P_{die} was also examined, assuming its values of 0–1. The other parameters were as given in the preceding paragraph. For the next simulations, we decided to keep $P_{die} = 0.01$, like in the previous work [19].

The influence of $R_{dif}A$ and initial V was checked for several I_{GS}/A and P_{break} values. This influence is nontrivial and deserves more attention in a future work. For the presented simulations, we assumed $R_{dif}A = 200$ and $V = 0$ as the initial value. The focus is on the role of the two other parameters. Preliminary simulations were conducted for P_{break} in range 0.1–0.3, and $I_{GS}/A = 5 \cdot 10^{-5} - -6 \cdot 10^{-4}$. Having gained some experience, for further simulations we select the parameter values that seem most likely to produce interesting behavior.

Data collected from the simulations are mainly V and I values as functions of time. For selected simulations, surface morphologies at chosen moments of time are rendered as snapshots, mainly in order to analyse the connection between the layer morphology and the potential oscillation stage. This connection is shown in Fig. 2 on an example of a system's evolution at $P_{break} = 0.15$ and $I_{GS}/A = 2 \cdot 10^{-4}$. Here, we can notice that high potential corresponds to high coverage of metal by the oxide.

3.1 Impact of Current and Adhesive Forces

The plots in Fig. 3 show how the overall behavior of the system depends on P_{break} and I_{GS}/A. Observed current is shown in the units of I_{GS}, so if it remains close to one, then it can be said that the galvanostat serves its purpose well. The plots

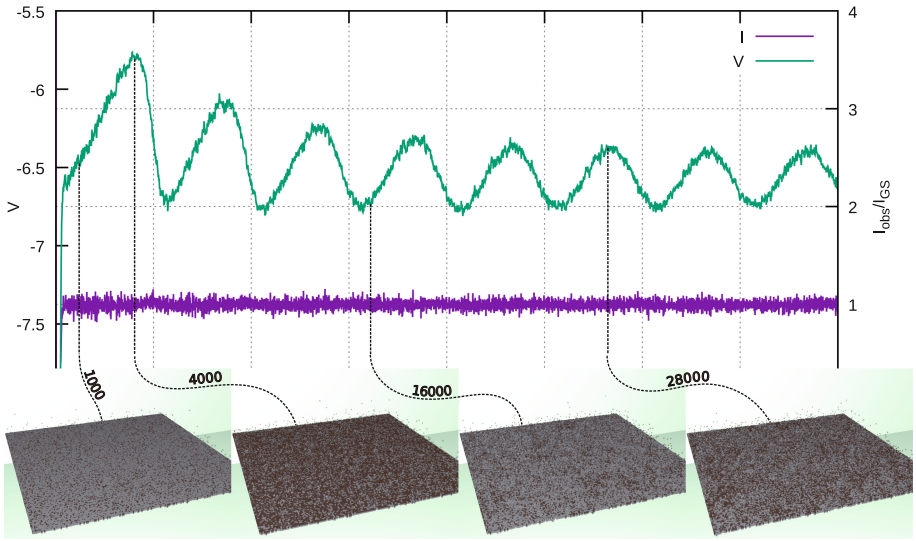

Fig. 2. Plot of time evolution of I (in purple) and V (green). observed current is divided by I_{GS}. Below the plot, shown are images of the metal surface at time $t \in \{1000, 4000, 16000, 28000\}$. Metal is rendered in light gray, oxide – in dark brown. (Color figure online)

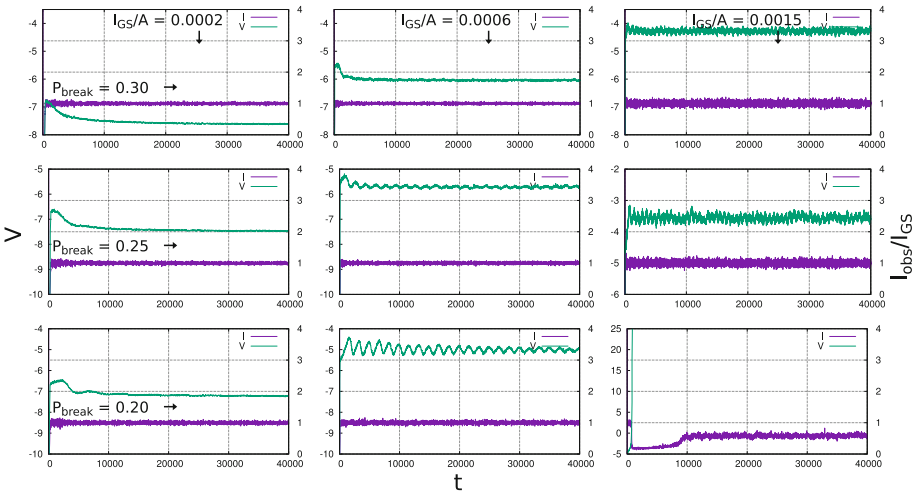

Fig. 3. Comparison of I and V evolution in time, for $I_{GS}/A \in \{2 \cdot 10^{-4}, 6 \cdot 10^{-4}, 1.5 \cdot 10^{-3}\}$ (left to right), $P_{break} \in \{0.3, 0.25, 0.2\}$ (top to bottom). Observed modes of behavior include: convergence to a steady state (left), stable oscillations of V (esp. central plot), damped oscillations (bottom central), chaotic oscillations (middle right) and passivation (bottom right plot).

show smooth convergence to a steady state, then damped, stable and chaotic oscillations, and passivation (saturation), when the potential grows rapidly, but no longer has any influence on the current, which stays below the target value. Those regimes occur approximately in the order of rising I_{GS}/A or falling P_{break}.

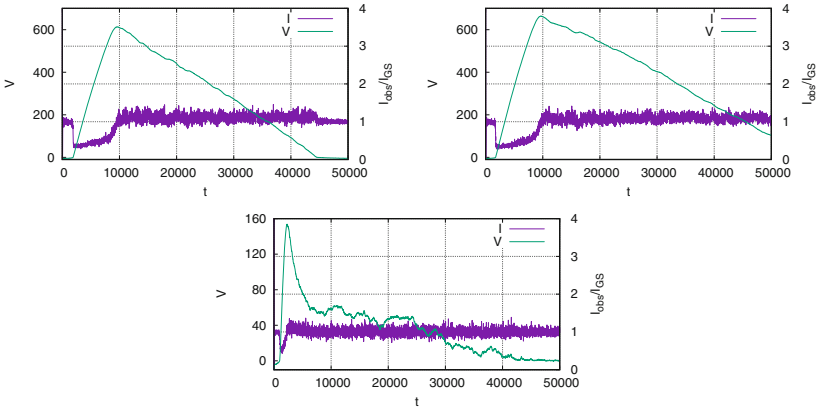

Fig. 4. Examples of I and V evolution in time, showing depassivation. Top: $P_{break} = 0.2$, with $I_{GS}/A = 7.75{\cdot}10^{-4}$ (left) and $8{\cdot}10^{-4}$ (right). Bottom: $P_{break} = 0.25$ and $I_{GS}/A = 1.8{\cdot}10^{-3}$. Depassivation occurs about $t = 10000$ (top) and 2000 (bottom).

Another phenomenon that can be observed in the simulations is the depassivation, when after a period of passivity the oxide layer becomes less compact and the current as set or greater starts flowing again. This can be seen in the I and V versus time plots, in Fig. 4. As we can see, the most interesting nonlinear behavior of the system occurs when the I_{GS} value is close to I_{max} – the maximum current that can be maintained for an arbitrarily long time. I_{max} obviously depends on all of the other parameters. It is difficult to calculate its value precisely, mostly due to the stochasticity of the model. When $I_{GS} \lesssim I_{max}$, we observe chaotic potential oscillations or passivation with subsequent depassivation.

4 Conclusions

We simulate passivation of metal in an electrolyte solution using a three-dimensional asynchronous stochastic cellular automaton as model. The model is taken from our earlier work, and coupled with a simple galvanostat, which changes the electric potential with a rate that is directly proportional to the difference between the desired and observed current. In the beginning of the research it was not obvious whether the oscillations could be obtained in our simulations. It could have been speculated, for example, that the time scale of the oscillations is too small related to the automaton's time step. Such doubts, however, appear to be unfounded. In fact, no modifications to the originally

assumed model are required. All of the results are obtained just by varying the values of the parameters – mostly the galvanostat current setting and the oxide adhesion strength, expressed in terms of P_{break}. To our knowledge, at the time of writing this paper, the presented model is the only one that mimics the salient features of passivation in so much detail. The simulated oscillatory patterns are still simpler and less varied, than those seen in the experiments – compare e.g. [15,17]. Thus, there is still room for improvement.

In general, the simulation studies on the passivation in galvanostatic conditions are far from over. More simulations are going to be conducted to explore the influence of the parameters in more detail, especially the sensitivity of the galvanostat. Future research includes also topological description of the oxide layers, modelling of the influence of aggressive anions (Cl^-, F^-) on passivation, and the influence of boundary conditions (periodic conditions are assumed in this paper). Following that, passivation in potentiodynamic and galvanodynamic conditions is going to be simulated. Hypothetically, using an appropriate potential or current protocol can result in the corrosion product forming curious nanostructures.

Acknowledgements. The authors need to thank the National Science Centre (Poland) for funding – OPUS Project: Numerical simulations of passive layer morphology at the metal electrode, grant number *UMO-2015/19/B/ST4/03753*.

References

1. Bandman, O.: Parallel simulation of asynchronous cellular automata evolution. In: El Yacoubi, S., Chopard, B., Bandini, S. (eds.) ACRI 2006. LNCS, vol. 4173, pp. 41–47. Springer, Heidelberg (2006). https://doi.org/10.1007/11861201_8
2. Bandman, O.: Coarse-grained parallelization of cellular-automata simulation algorithms. In: Malyshkin, V. (ed.) PaCT 2007. LNCS, vol. 4671, pp. 370–384. Springer, Heidelberg (2007). https://doi.org/10.1007/978-3-540-73940-1_38
3. Bartosik, Ł.: Simulation of nanostructured surfaces obtained by passivity and growth. Ph.D. thesis, Institute of Physical Chemistry, Polish Academy of Sciences, Warsaw, Poland (2014)
4. Bartosik, Ł., Stafiej, J., di Caprio, D.: 3D simulations of ordered nanopore growth in alumina. Electrochim. Acta **188**, 218–221 (2016). https://doi.org/10.1016/j.electacta.2015.08.164
5. di Caprio, D., Stafiej, J.: Simulations of passivation phenomena based on discrete lattice gas automata. Electrochim. Acta **55**, 3884–3890 (2010). https://doi.org/10.1016/j.electacta.2010.01.106
6. di Caprio, D., Stafiej, J.: The role of adsorption in passivation phenomena modelled by discrete lattice gas automata. Electrochim. Acta **56**, 3963–3968 (2011). https://doi.org/10.1016/j.electacta.2011.02.018
7. di Caprio, D., Stafiej, J., Luciano, G., Arurault, L.: 3D cellular automata simulations of intra and intergranular corrosion. Corros. Sci. **112**, 438–450 (2016). https://doi.org/10.1016/j.corsci.2016.07.028
8. Chen, S., Guillemot, G., Gandin, C.A.: Three-dimensional cellular automaton-finite element modeling of solidification grain structures for arc-welding processes. Acta Mater. **115**, 448–467 (2016). https://doi.org/10.1016/j.actamat.2016.05.011

9. Lhuissier, P., de Formanoir, C., Martin, G., Dendievel, R., Godet, S.: Geometrical control of lattice structures produced by EBM through chemical etching: investigations at the scale of individual struts. Mater. Des. **110**, 485–493 (2016). https://doi.org/10.1016/j.matdes.2016.08.029
10. Li, H., Sun, X., Yang, H.: A three-dimensional cellular automata-crystal plasticity finite element model for predicting the multiscale interaction among heterogeneous deformation, DRX microstructural evolution and mechanical responses in titanium alloys. Int. J. Plast. **87**, 154–180 (2016). https://doi.org/10.1016/j.ijplas.2016.09.008
11. Pagitsas, M., Pavlidou, M., Sazou, D.: Localized passivity breakdown of iron in chlorate- and perchlorate-containing sulphuric acid solutions: a study based on current oscillations and a point defect model. Electrochim. Acta **53**, 4784–4795 (2008). https://doi.org/10.1016/j.electacta.2008.01.065
12. Pavlidou, M., Pagitsas, M., Sazou, D.: Potential oscillations induced by the local breakdown of passive iron in sulfuric acid media. An evaluation of the inhibiting effect of nitrates on iron corrosion. J. Solid State Electrochem. **19**(11), 3207–3217 (2015). https://doi.org/10.1007/s10008-015-2812-0
13. Pérez-Brokate, C.F., di Caprio, D., Mahé, E., Féron, D., de Lamare, J.: Cyclic voltammetry simulations with cellular automata. J. Comput. Sci. **11**, 269–278 (2015). https://doi.org/10.1016/j.jocs.2015.08.005
14. Popova, E., Staraselski, Y., Brahme, A., Mishra, R., Inal, K.: Coupled crystal plasticity - probabilistic cellular automata approach to model dynamic recrystallization in magnesium alloys. Int. J. Plast. **66**, 85–102 (2015). https://doi.org/10.1016/j.ijplas.2014.04.008
15. Sazou, D., Kominia, A., Pagitsas, M.: Corrosion processes of iron in acidic solutions associated with potential oscillations induced by chlorates and perchlorates. J. Solid State Electrochem. **18**, 347–360 (2014). https://doi.org/10.1007/s10008-013-2244-7
16. Sazou, D., Michael, K., Pagitsas, M.: Intrinsic coherence resonance in the chloride-induced temporal dynamics of the iron electrodissolution-passivation in sulfuric acid solutions. Electrochim. Acta **119**, 175–183 (2014). https://doi.org/10.1016/j.electacta.2013.12.029
17. Sazou, D., Pavlidou, M., Pagitsas, M.: Potential oscillations induced by localized corrosion of the passivity on iron in halide-containing sulfuric acid media as a probe for a comparative study of the halide effect. J. Electroanal. Chem. **675**, 54–67 (2012). https://doi.org/10.1016/j.jelechem.2012.04.012
18. Sikora, E., Macdonald, D.D.: Defining the passive state. Solid State Ionics **94**, 141–150 (1997)
19. Stępień, J., di Caprio, D., Stafiej, J.: 3D simulation studies of the metal passivation process. Electrochim. Acta (submitted)
20. Uhlig, H.H.: Passivity in metals and alloys. Corros. Sci. **19**(7), 777–791 (1979). https://doi.org/10.1016/S0010-938X(79)80075-X
21. Yang, F., Huang, L., Guo, T., Wang, C., Wang, L., Zhang, P.: The precise preparation of anodic aluminum oxide template based on the current-controlled method. Ferroelectrics **523**, 50–60 (2018). https://doi.org/10.1080/00150193.2018.1391540